JURNAL KIMIA (*JOURNAL OF CHEMISTRY*) 19 (2), JULI 2025 **p-ISSN 1907-9850**
DOI: https://doi.org/10.24843/JCHEM.2025.v19.i02.p03 **e-ISSN 2599-2740**

SYNTHESIS AND CHARACTERIZATION OF $BiVO_4$ AND Co-DOPED $BiVO_4$ FILMS AS PHOTOCATALYST MATERIAL

K. Adhaina, F. Failamani, B. Prijamboedi*

Department of Chemistry, Faculty of Mathematics and Natural Science, Bandung Institute of Technology, Jl. Ganesha 10, Bandung 40132, Indonesia
****Email: prijamboedi@itb.ac.id***

Article Received on: 23th January 2025 Revised on: 20th May 2025 Accepted on: 1st July 2025

ABSTRAK

Bismut vanadat ($BiVO_4$) merupakan semikonduktor tipe-n dengan energi celah pita sebesar 2,4 eV karena adanya perbedaan energi antara orbital *6s* Bi^{3+} dan orbital *3d* V^{5+}. Energi celah pita yang sempit ini membuat $BiVO_4$ mampu menyerap cahaya tampak, sehingga menjadikannya kandidat potensial sebagai material fotokatalis. Namun, kinerja fotokatalitik $BiVO_4$ terbatas karena mobilitas elektron yang rendah dan laju rekombinasi pasangan elektron-lubang yang tinggi, sehingga menurunkan efektivitas fotokatalitiknya. Modifikasi material diperlukan untuk menghambat rekombinasi elektron-lubang, salah satunya melalui doping dengan kobalt (Co^{2+}) pada permukaan $BiVO_4$ berfungsi sebagai perangkap muatan. Dalam penelitian ini, film $BiVO_4$ disintesis menggunakan bubuk $BiVO_4$ yang diperoleh melalui metode hidrotermal. Asam sitrat digunakan sebagai prekursor, sementara etilen glikol digunakan sebagai *binder* dan pelarut. Untuk film $BiVO_4$ terdoping Co, ion Co^{2+} didispersikan ke permukaan film $BiVO_4$ dengan menambahkan larutan kobalt(II) nitrat ke permukaan film yang telah disiapkan sebelumnya. Analisis pola difraksi sinar-X (XRD) menunjukkan bahwa film $BiVO_4$ memiliki polikristalin dengan struktor monoklinik Scheelite. Selain itu, terdapat preferensi orientasi kristal pada arah <040>. Karakterisasi sifat optik menggunakan spektroskopi reflektansi difusi UV-vis menunjukkan bahwa energi celah pita (Eg) untuk transisi elektronik yang diizinkan secara langsung sebesar 2,49 eV, yang dihitung menggunakan metode Kubelka-Munk. Film $BiVO_4$ terdoping kobalt memperlihatkan dua tepi serapan tambahan pada 2,28 eV dan 1,45 eV, yang mengindikasikan keberadaan keadaan cacat (*defect states*) yang berasal dari penggabungan ion kobalt pada permukaan film. Hasil penelitian ini menunjukkan bahwa sifat optik dan struktural film $BiVO_4$ sangat dipengaruhi oleh teknik sintesis yang digunakan.

Kata Kunci: $BiVO_4$, $BiVO_4$ terdoping Co, sifat optik, film.

ABSTRACT

Bismuth vanadate (BiVO4) is an n-type semiconductor material with a narrow energy gap of 2.4 eV, due to the difference between the energy level of the 6s orbital of Bi^{3+} and the 3d orbital of V^{5+}. Its narrow band gap is suitable for photocatalytic processes in the visible light region, but the low electron mobility and high electron-hole recombination rate reduce its photocatalytic effectiveness. Modification of this material is necessary to prevent electron-hole recombination, and it can be carried out by introducing Co^{2+} on the surface of BiVO4 as a charge trap. In this study, BiVO4 and cobalt-doped BiVO4 films were prepared by using hydrothermally synthesized BiVO4 powder, citric acid, and ethylene glycol as precursor, binder, and solvent, respectively. For cobalt-doped BiVO4 films, Co^{2+} ions were added onto BiVO4 films by spreading the cobalt(II) nitrate solution on the surface of the prepared BiVO4 films. The X-ray diffraction (XRD) patterns of the films indicated that they were polycrystalline with a monoclinic scheelite crystal structure. Moreover, preferred growth along the <040> directions was observed in the films. The optical properties of the films were analyzed by UV-Vis diffuse reflectance spectroscopy. The optical energy gap (Eg) of the deposited films was estimated using the Kubelka-Munk plot, and the value was 2.49 eV for the direct allowed electronic transition. The Co-doped BiVO4 films showed two absorption edges at 2.28 and 1.45 eV, which indicated the presence of defect states originating from the cobalt incorporation on the surface. These results indicated that the properties of BiVO4 films are highly affected by the preparation technique.

Keywords: $BiVO_4$, cobalt doped $BiVO_4$, optical properties, films.

INTRODUCTION

Photocatalysis is a process that promotes chemical reactions by utilizing photon energy mediated by semiconductor materials called photocatalysts and introduces reactive species. When the photocatalyst is exposed to sufficient light radiation, electrons from the valence band will be excited to the conduction band, leaving holes in the valence band, and thus creating electron-hole. The photogenerated electron-hole pairs are furthermore involved in various redox reactions (Náfrádi et al., 2022). This material has attracted significant attention because of its potential applications in environmental remediation (Noureen et al., 2023), energy conversion (Yaghoubi et al., 2024), and organic synthesis (Akita et al., 2023). Although photocatalysis are simple, affordable, and scalable, their efficiency is still considered lacking in application. Therefore, to achieve higher photocatalysis efficiency, it is necessary to improve its physical properties such as redox potential, number of reaction sites, and photogenerated carrier flow (Oktariza et al., 2024).

Among various semiconductors, bismuth vanadate ($BiVO_4$) is a promising photocatalyst material. Besides its non-toxic nature and resistant to chemical corrosion, this compound also has a band gap energy of ~2.4 eV, making it is suitable to operate in the visible light region ($\lambda \cong 500$ nm). Bismuth vanadate has three types of crystal structures, which are monoclinic scheelite (m-s), tetragonal scheelite (t-s), and tetragonal zirconia (t-z) structures. Among these structures, the monoclinic scheelite (m-s) structure is considered to have better photocatalytic activity because it has a narrow energy gap. Density Functional Theory (DFT) calculation showed that the valence band of $BiVO_4$ is mainly composed of 6s orbital of Bi^{3+}, while the conduction band is composed of the 3d orbital of V^{5+} (Hajra et al., 2019; da Silva et al., 2012). In addition, the valence band (VB) edge is in the vicinity of the oxidation potential value of water, which is favorable for the formation of reactive oxygen species such as $\bullet O_2^-$, H_2O_2 and •OH (Hernández et al., 2015; Lebedev et al., 2020]. Despite the mentioned advantages, the photocatalytic activity of $BiVO_4$ is hampered by the high rate of charge carrier recombination caused by the low mobility of electrons (Oktariza et al., 2024). Moreover, the application of $BiVO_4$ powder as photocatalyst in the aqueous phase makes it to be difficult to recollect, thus reducing its reusability (Hajra et al., 2019).

In this study, we aim to improve the photocatalytic activity of $BiVO_4$ via surface modification by incorporation of Co^{2+} ions. Cobalt is chosen since the energy level of the 3d orbital of Co^{2+} is lower than that of the 3d orbital of V^{5+}, therefore they can act as electron traps and prevent electron-hole recombination. The $BiVO_4$ films were prepared by coating using the doctor blade technique (Huang et al., 2023). This simple and inexpensive deposition technique could produce consistent and uniform layers (Huang et al., 2024). The powder and film samples were characterized by X-ray diffraction (XRD), which determines its crystal structure. Optical characterization was carried out with UV-Vis diffuse reflection spectrometer to obtain the energy gap values.

MATERIALS AND METHODS

Synthesis of $BiVO_4$ and Surface Modification

The $BiVO_4$ bulk material was prepared using the hydrothermal method. At first, 3 mmol $Bi(NO_3)_3.5H_2O$ and 3 mmol NH_4VO_3 were dissolved in a 2 M HNO_3 solution. Then, the pH was adjusted by adding 25% w/v NH_3 solution until it reached pH 1.5 - 2.0, and a yellow suspension was formed. The suspension was subsequently transferred into a Teflon-lined stainless-steel autoclave and heated in an oven at 200 ºC for 24 hours. The yellow powder was separated by filtration and rinsed with demineralized water. Finally, the powder was dried in an oven at 65 ºC for 24 hours. Surface modifications were prepared by mixing $Co(NO_3)_2.6H_2O$ and $BiVO_4$ with a mole ratio of Co^{2+} ions to $BiVO_4$ of 1:20. The mixture was dissolved in demineralized water and stirred at a solution temperature of ~65 ºC to evaporate the water until it dry. Then, the powder was calcined in a furnace at a temperature of 300 ºC for 4 hours.

Preparation of Co-doped $BiVO_4$ film

The $BiVO_4$ films were prepared using the doctor blade method (Huang et al., 2023). First, $BiVO_4$ paste was prepared by dissolving 1.3 mmol citric acid into 5 mL demineralized water and then stirred at 70 ºC for 30 minutes. The mixture was added with 7.8 mmol ethylene glycol gradually and stirred until homogeneous

and then 1.3 mmol $BiVO_4$ was added. The mixture was stirred at ~110 ºC for 70 minutes and continued at 65 ºC for 24 hours. The glass substrates were prepared by washing it with detergent, soaking in ethanol, and the drying at 110 ºC for 2 hours. The precursor paste was deposited on a 25.4 x 76.2 mm^2 glass substrate with a thickness of 1 mm - 1.5 mm via the doctor blade method. The film was dried in a hotplate at 80 - 210 ºC for 4 hours. The $BiVO_4$ film surface modification was prepared by spreading 1 mL of 0.1 M $Co(NO_3)_2$ solution on the surface of the $BiVO_4$ film until it was evenly distributed by the blade. The film was dried on a hotplate at 65 °C for 2 hours, followed by calcination at 300 °C for 8 hours.

Characterizations

The crystalline phase of $BiVO_4$ and Co-doped $BiVO_4$ bulk and film was identified by X-ray diffraction analysis using X Rigaku xtaLAB mini II Diffractometer with CuKα source (λ = 1.54059 Å) with the 2θ range of 10 - 90°. Lattice parameter and Miller index (hkl) analysis were performed using the Rietveld refinement method using Fullprof suite software (Altalhi et al., 2021). The crystallite sizes of the samples were estimated using the Scherrer equation. UV-Vis diffuse reflectance spectra were measured using a UV-Vis Thermo Scientific Evolution 220 spectrophotometer. The direct and indirect allowed band gaps (E_g) energy were calculated using the Kulbeka-Munk function and the Tauc plot.

RESULTS AND DISCUSSION

The X-ray diffraction method was used to analyze the crystal structure of the bulk and film of $BiVO_4$. The XRD patterns obtained for the bulk and film are presented in Figure 1 (a). It can be seen that the $BiVO_4$ samples adopt a monoclinic crystal structure with a space group of *C*2/*c*. There is no significant difference between the diffraction pattern of the bulk and film of $BiVO_4$. Based on the refinement results shown in Table 1, the lattice parameters of our sample increased compared to the previously reported sample (Zhao et al., 2011). However, the lattice parameters after modification with Co^{2+} only slightly changed. Also, the diffraction peak position did not change, as shown in Figure 1 (b). This fact confirmed our hypothesis that cobalt does not enter the crystal lattice and only stays on the surface. For the crystallite size, the calculated values, which were determined using the Scherrer equation, are also reported in Table 1. The crystallite size of the $BiVO_4$ bulk was 28.45 nm, while after surface modification with Co^{2+}, it increased by 28.61 nm. Figure 2 shows the intensity ratio of the (130) to (040) crystal reflection planes of $BiVO_4$ and Co-doped $BiVO_4$. The film shows an increase in the intensity of the (040) crystal plane compared to the bulk. It can be concluded that crystal grains grow towards the b-axis in the film, indicating a preferred orientation or a possibility of different growth orientation.

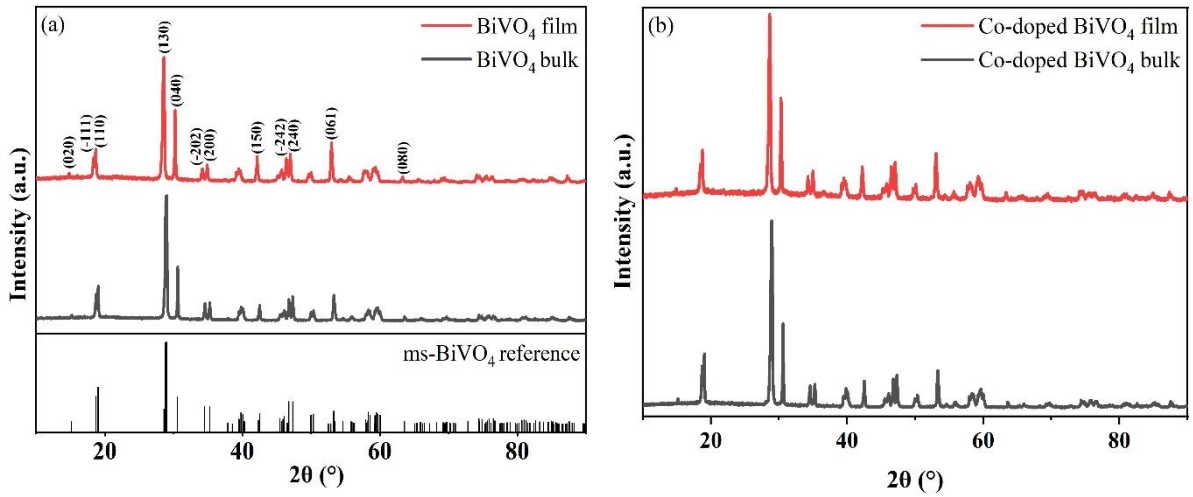

Figure 1. X-ray Diffraction Patterns of $BiVO_4$ (a) and Co-doped $BiVO_4$ (b) Bulk and Film.

Table 1. Crystallite Size and Lattice Parameter of $BiVO_4$ and Co-doped $BiVO_4$ Bulk.

	Crystallite Size (nm)	Lattice Parameter a (Å)	b (Å)	c (Å)	β (°)	Cell Volume (Å^3)
$BiVO_4$ (ref)	20-30	7.224	11.522	5.108	135.003	425.164
$BiVO_4$ (exp)	28.45	7.298	11.698	5.194	135.754	443.509
Co-doped $BiVO_4$ (exp)	28.61	7.301	11.701	5.195	135.739	443.832

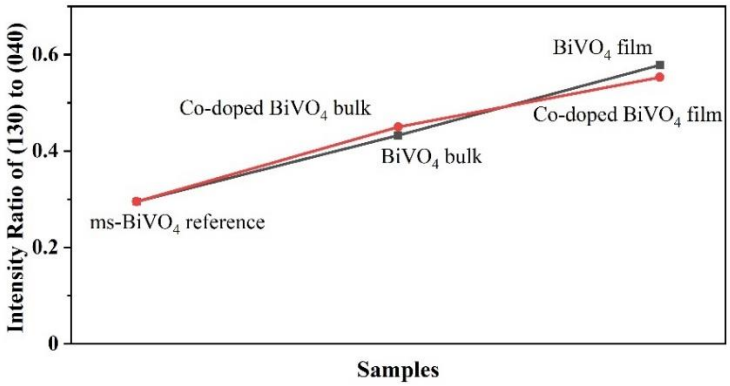

Figure 2. The Intensity Ratio of (130) and (040) Diffraction Peaks of Bulk and Film.

To probe the electronic states of the $BiVO_4$ semiconductor materials, the diffuse reflectance spectrometer (DRS) was used. Figure 3 (a) shows the diffuse reflection spectra of $BiVO_4$ bulk and film. $BiVO_4$ bulk shows high reflectance in the visible to IR region (above 500 nm). Below 500 nm, there is a strong absorbance, and it is related to the band-to-band transition. However, the spectrum of $BiVO_4$ films shows a decrease in reflectance starting from the IR region (~900 nm). This indicates the possibility of transitioning with energy below the band gap, originating from several in-gap states. The presence of the in-gap states could be related to the process of thin film preparation. Further experiments are required to clarify these issues.

In contrast to the undoped $BiVO_4$, both bulk and film of Co-doped $BiVO_4$ show significant absorbance starting from the IR region, as shown in Figure 3 (b). The strong absorbance near 500 nm, corresponding to the band-to-band transition, became less pronounced than in the undoped samples. Moreover, another strong absorbance occurred near the wavelength of ~800 nm, which could be attributed to the presence of Co^{2+} on the surface. However, in the Co-doped $BiVO_4$ film, the reflectance is lower than that of the bulk; it is thought that there is an increased surface roughness compared to bulk materials. This roughness can lead to enhanced light scattering and trapping within the film, reducing the amount of reflected light (Bakhtiarnia et al., 2022). The band gap of bulk and films was calculated by the Kubelka-Munk function (F(R)) as follows:

$$F(R)= \frac{K}{S} = \frac{(1-R)^2}{2R} \quad (1)$$

$$[E \times F(R)]^n = A(E-E_g) \quad (2)$$

Where E is the photon energy; E_g is the band gap energy; K is absorption; S is back-scattering coefficients, and n is a constant determined by the semiconductor, that is a direct band gap for n = 2 and an indirect band gap for n = 1/2, respectively. Figure 4 shows the plot of $[E \times F(R)]^n$ versus photon energy of the energy band gap of $BiVO_4$ bulk and films. The linear regime of the Tauc plots indicates the band gap transition, where the intercept at the x-axis (energy) measures the band gap energy. The resulting band gap value in $BiVO_4$ bulk is 2.41 eV and 2.35 eV for the direct and indirect allowed transition, respectively. While the direct allowed band gap of $BiVO_4$ bulk and film did not show a significant difference, the indirect allowed band gap increased

significantly from 2.35 eV to 2.43 eV. Moreover, we observe a slight increase in absorbance with energy below the band gap. These results are in good agreement with published reports for the synthesis of bulk and thin films obtained by other techniques (Zhou et al., 2011), confirming the presence of in-gap states in the undoped $BiVO_4$ films.

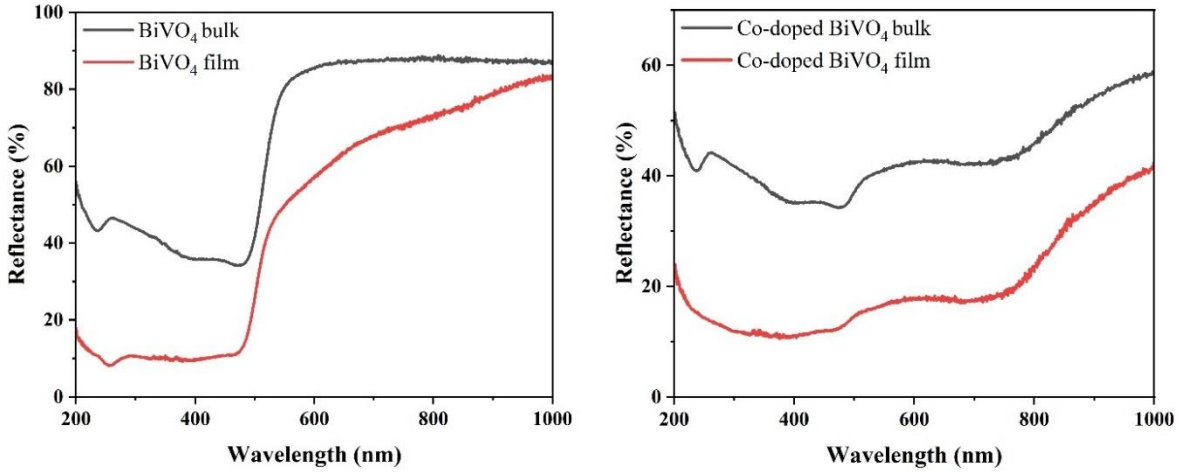

Figure 3. UV-vis Diffuse Reflection Spectra of $BiVO_4$ (a) and Co-doped $BiVO_4$ (b) Bulk and Film.

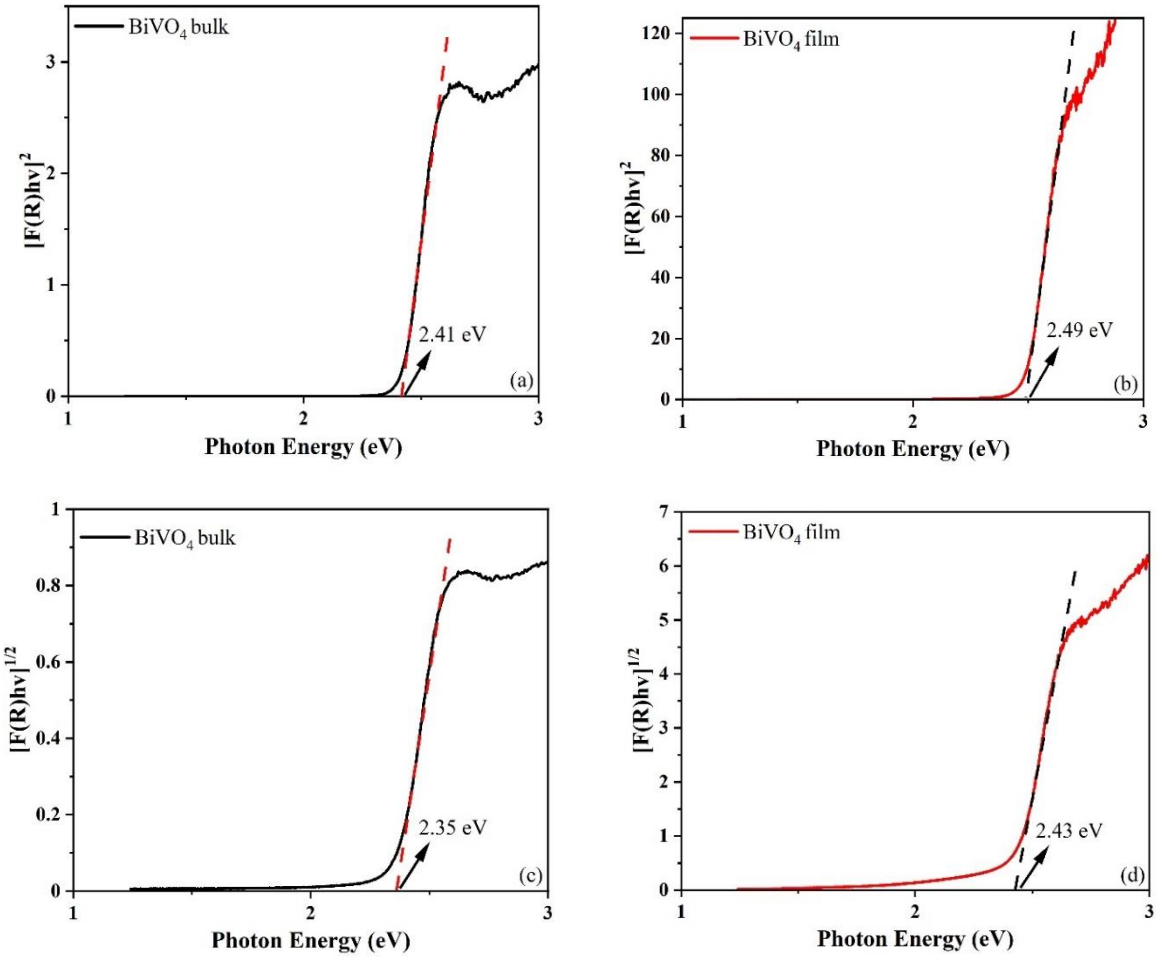

Figure 4. The Tauc Plot for The Energy Band Gap of $BiVO_4$ Bulk (a) And Film (b) in Direct Allowed Transition and $BiVO_4$ Bulk (c) And Film (d) Indirect Allowed Electronic Transition

Figure 5 shows the Tauc-plot of $BiVO_4$ after surface modification with Co^{2+}. Both direct and indirect band gaps of Co-doped $BiVO_4$ decrease in the bulk and film forms compared to the undoped ones. An additional transition is observed below the band-to-band transition, which originated from the Co^{2+} on the surface. Like the indirect transition in the undoped $BiVO_4$, we also observe a significant increase in absorbance below the band gap value. This confirms that the presence of Co^{2+} increases the number of in-gap states in the Co-doped $BiVO_4$. In bulk, the band gap energy of Co-doped $BiVO_4$ is 2.29 eV a nd 2.07 eV at direct and indirect allowed electronic transition, respectively. However, the effect of defects causes the formation of band tails (E_{g2}) of 1.38 eV and 1.29 eV at direct and indirect allowed. The Co-doped $BiVO_4$ film shows the similarity of band gap energy plot with bulk. It exhibits two absorption edges at 2.28 and 2.02 eV. Meanwhile, the secondary band gap energy (E_{g2}) decreased in the film to 1.45 eV and 1.34 eV, creating a broader band gap. The presence of the in-gap states could act as carrier traps, which reduces the charge carrier recombination rate. Therefore, we expect the photocatalytic performance of the films, both doped and undoped, will be higher than the bulk.

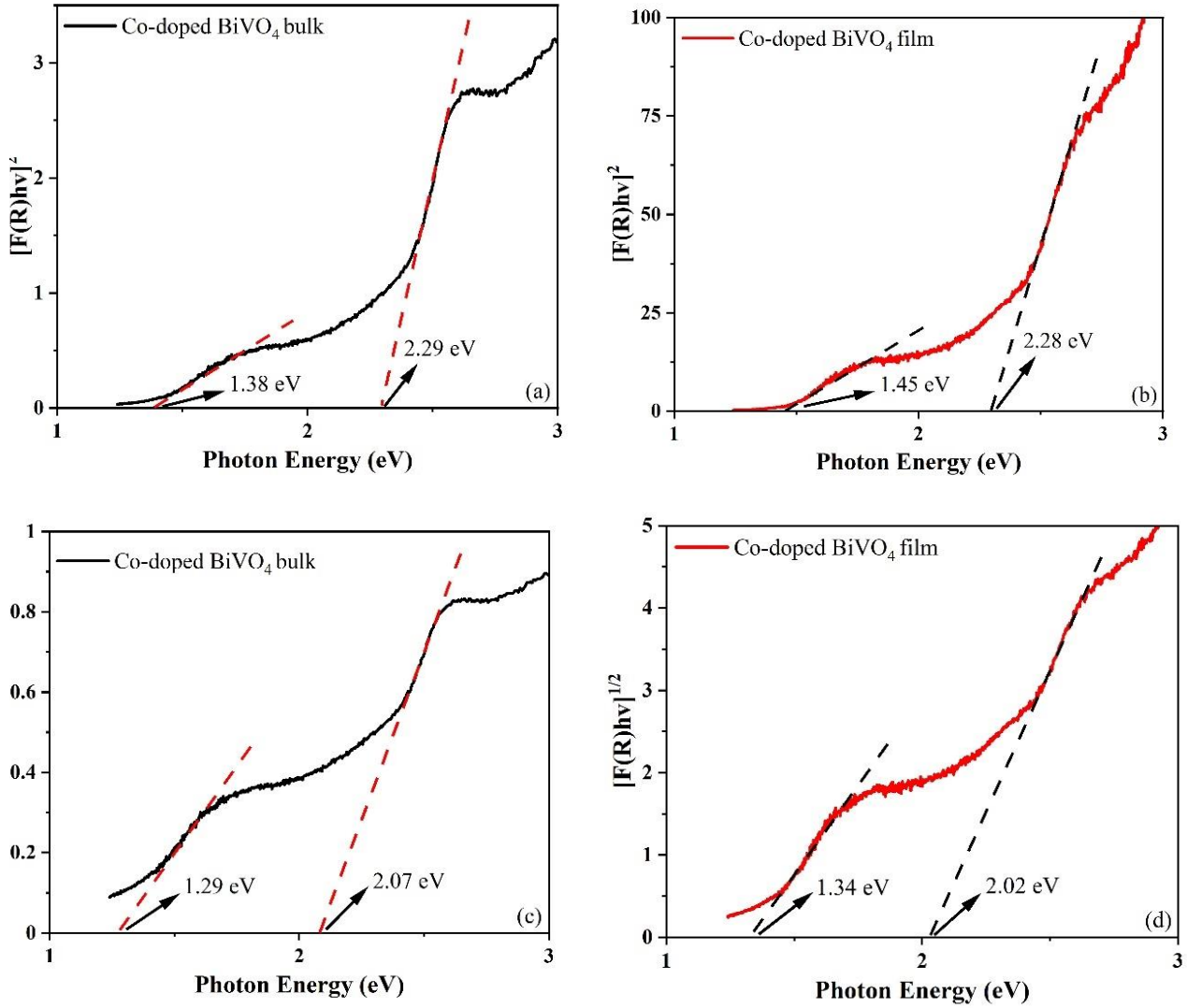

Figure 5. A Tauc's Plot for The Energy Band Gap of Co-doped $BiVO_4$ Bulk (a) and Film (b) in Direct Allowed Transition and Co-doped $BiVO_4$ Bulk (c) and Film (d) Indirect Allowed Electronic Transition.

CONCLUSIONS

The structure and electronic structure properties of $BiVO_4$ and Co-doped $BiVO_4$ of bulk and film were studied. The synthesized and coated to glass substrate samples retained a monoclinic scheelite structure. We observed no significant change in the diffraction peaks of the bulk and film samples. However, UV-vis diffuse reflection spectra suggested that the absorption edge of $BiVO_4$ bulk and films started from 450 nm, with a corresponding band gap of 2.41 and 2.49 eV, respectively. The introduction of cobalt induced crystal defects and created a band tail. The Co-doped samples showed two absorption edges at 2.29 and 1.38 eV for bulk and 2.28 and 1.45 eV for films and direct allowed electronic transition for films which slightly reduce the main gap and create defect start at around 1.4 eV. This indicated the presence of defect states originating from the cobalt incorporation on the surface. These results showed that the properties of BiVO4 films are highly affected by the preparation technique.

REFERENCES

Náfrádi, M., Veréb, G., Firak, D.S., Alapi, T. 2022. *Photocatalysis: Introduction, Mechanism, and Effective Parameters*. in: Garg, S., Chandra, A. (Eds.), *Green Photocatalytic Semiconductors. Green Chemistry and Sustainable Technology.* Springer: Cham: 3-31.

Noureen, A., Wang, Q., Humayun, M., Shah, W. A., Xu, Q., Wang, X. 2023. Recent advances in structural engineering of photocatalysts for environmental remediation. *Environmental Research*. 219:115084.

Yaghoubi, S., Mousavi, S. M., Babapoor, A., Binazadeh, M., Lai, C. W., Althomali, R. H., Rahman, M. M., Chiang, W. H. 2024. Photocatalysts for solar energy conversion: Recent advances and environmental applications. *Renewable and Sustainable Energy Reviews*. 200: 114538.

Akita, M., Ceroni, P., Stephenson, G. Masson. 2023. Progress in Photocatalysis for Organic Chemistry. *The Journal of Organic Chemistry*. 88(10): 6281-6283.

Oktariza, L. G., Sato, Y., Gofurov, S., Ozawa, K., Islam, M. M., Ikeda, S., Sakurai, T. 2024. Characterization of the electronic structure of sputter-deposited Mo-doped $BiVO_4$ thin-film photoanodes. *Japan Journal of Applied. Physics.* 63: 02SP41.

Hajra, P., Kundu, S., Maity, A., Bhattacharya, C. 2019. Facile photoelectrochemical water oxidation on Co^{2+}-adsorbed $BiVO_4$ thin films synthesized from aqueous solutions. *Chemical Engineering Journal*. 374: 1221-1230.

da Silva, M. R., Dall Antonia, L. H., Scalvi, L. V. A., dos Santos, D. I., Ruggiero, L. O., Urbano, A. 2012. Deposition and characterization of $BiVO_4$ thin films and evaluation as photoanodes for methylene blue degradation. *Journal of Solid-State Electrochemistry*. 16: 3627.

Hernández, S., Thalluri, S. M., Sacco, A., Bensaid, S., Saracco, G., Russo, N. 2015. Photo-catalytic activity of $BiVO_4$ thin-film electrodes for solar-driven water splitting. *Applied Catalysis A:* General. 504: 266-271.

Lebedev, A., Anariba, F., Li, X., Wu, P. 2020. Rational design of visible-light-sensitive Ag-$BiVO_4$ oxides by matching redox potentials of catalyst, dyes, and reactive oxygen species towards more efficient photocatalytic degradation. *Journal of Environmental Chemical Engineering*. 8(3): 103748.

Huang, K. W., Li, M. H., Chen, Y. T., Wen, Z. X., Lin, C. F., Chen, P. 2024. Fast fabrication of μm-thick perovskite films by using a one-step doctor-blade coating method for direct X-ray detectors. *Journal of Materials Chemistry C*. 12(4): 1533-1542.

Altalhi, T., Gobouri, A.A., Al-Harbi, L. M., Refat, M. S., El-Nahass, M.M., Hassanien, A.M., Atta, A.A., Ahmed, E. M. A. 2021. Structural, diffuse reflectance spectroscopy and dielectric relaxation properties of zirconium (IV) dioxide. *Journal of Materials Research and Technology*. 12: 1194-1202.

Zhao, Z., Li, Z., Zou, Z. 2011. Electronic structure and optical properties of monoclinic clinobisvanite $BiVO_4$. *Physical Chemistry Chemical Physics*. 13(10): 4746-4753.

Bakhtiarnia, S., Sheibani, S., Billard, A., Aubry, E., Yazdi, M. A. P. 2022. Deposition of nanoporous $BiVO_4$ thin film photocatalyst by reactive magnetron sputtering: Effect of total pressure and substrate. *Transactions of Nonferrous Metals Society of China*. 32(3): 957-971.

Zhou, B., Qu, J., Zhao, X., Liu, H. 2011. Fabrication and photoelectrocatalytic properties of nanocrystalline monoclinic $BiVO_4$ thin-film electrode. *Journal of Environmental Sciences*. 23(1): 151-159.